Chromatin remodelers in the DNA double strand break response

Smeenk, G.

CHAPTER 5

RAD51C IS ESSENTIAL FOR EMBRYONIC DEVELOPMENT AND HAPLOINSUFFICIENCY CAUSES INCREASED DNA DAMAGE SENSITIVITY AND GENOMIC INSTABILITY

Godelieve Smeenk[a,c], Anton J.L. de Groot[a,c], Ron J. Romeijn[a], Paul P.W. van Buul[a], Malgorzata Z. Zdzienicka[b], Leon H.F. Mullenders[a], Albert Pastink[a] and Barbara C. Godthelp[a]

[a]Department of Toxicogenetics, Leiden University Medical Center, Leiden, postal zone S-4-P, P.O. Box 9600, 2300 RC Leiden, The Netherlands. [b]Department of Molecular Cell Genetics, L. Rydygier Collegium Medicum, N.Copernicus University,Ul. Sklodowskiej- Curie 9, 85-094 Bydgoszcz, Poland

[c]Both authors contributed equally to this work.

Published in Mutation Research 2010, Jul 7;689(1-2):50-58.

ABSTRACT

Homologous recombination is essential for repair of DNA interstrand cross-links and double-strand breaks. The Rad51C protein is one of the five Rad51 paralogs in vertebrates implicated in homologous recombination. A previously described hamster cell mutant defective in Rad51C (CL-V4B) showed increased sensitivity to DNA damaging agents and displayed genomic instability. Here, we identified a splice donor mutation at position +5 of intron 5 of the *Rad51C* gene in this mutant, and generated mice harbouring an analogous base-pair alteration. *Rad51C*^{splice} heterozygous animals are viable and do not display any phenotypic abnormalities, however homozygous *Rad51C*^{splice} embryos die during early development (E8.5). Detailed analysis of two CL-V4B revertants, V4B-MR1 and V4B–MR2, that have reduced levels of full-length *Rad51C* transcript when compared to wild type hamster cells, showed increased sensitivity to mitomycin C (MMC) in clonogenic survival, suggesting haploinsufficiency of *Rad51C*. Similarly, mouse *Rad51C*$^{splice/neo}$ heterozygous ES cells also displayed increased MMC sensitivity. Moreover, in both hamster revertants, *Rad51C* haploinsufficiency gives rise to increased frequencies of spontaneous and MMC-induced chromosomal aberrations, impaired sister chromatid cohesion and reduced cloning efficiency. These results imply that adequate expression of *Rad51C* in mammalian cells is essential for maintaining genomic stability and sister chromatid cohesion to prevent malignant transformation.

INTRODUCTION

Homologous recombination (HR) is a major pathway involved in the repair of double-strand breaks (DSBs) and interstrand cross-links (ICLs) in DNA and requires homologous sequences present on either a sister chromatid or homologous chromosome to accurately repair these lesions (Wyman and Kanaar, 2006). The initial steps in this process are dependent on Rad51, the central protein in HR, and several other factors belonging to the Rad52 epistasis group, including the Rad51 paralogs (Li and Heyer, 2008; San Filippo et al., 2008). In mammals five Rad51-like proteins have been identified, XRCC2, XRCC3, Rad51B, Rad51C and Rad51D (Thacker, 1999). The Rad51 paralogs share limited sequence homology with each other and with Rad51. Physical interactions have been observed among these five paralogs and two specific subcomplexes were identified: one containing XRCC2, Rad51B, Rad51C and Rad51D and the other XRCC3 and Rad51C (Li and Heyer, 2008; Thacker, 2005). Several of the paralogs are able to bind to single-strand DNA and display ATPase activity but little is known about the precise function of these proteins in HR. The redistribution of Rad51 to sites of DNA damage strongly depends on several proteins involved in HR including the Rad51 paralogs, Rad52, Rad54, RPA, BRCA1, BRCA2 and PALB2 (Godthelp et al., 2002a; Haaf et al., 1995; Tashiro et al., 2000; Xia et al., 2007). These observations suggest a role for the Rad51 paralogs at the early stages of recombination, presumably in the assembly and/or stabilization of Rad51 filaments as observed for Rad55 and Rad57, the two Rad51 paralogs in yeast (Sung, 1997). In addition to facilitating Rad51 filament assembly, Rad51C is required for efficient checkpoint signaling by promoting CHK2 phosphorylation to delay cell cycle progression in response to DNA damage (Badie et al., 2009) and the regulation of Rad51 ubiquitination and degradation (Bennett and Knight, 2005). A role for Rad51C at later stages in recombination is implied by the co-purification of Rad51C (and XRCC3) with protein fractions showing Holliday junction resolvase activity and the localization to mouse meiotic chromosomes at pachytene/diplotene (Liu et al., 2007). A role for Rad51 paralogs beyond the initiation of HR is also apparent from the analysis of recombination products in XRCC2, XRCC3 and Rad51C deficient hamster cells (Brenneman et al., 2002; Nagaraju et al., 2006; Nagaraju et al., 2009).

Disruption of Rad51 paralogs in chicken DT40 cells leads to increased sensitivity to cross-linking agents and defects in HR (Takata et al., 2001). However, in mice the absence of XRCC2, Rad51B, Rad51C or Rad51D is not tolerated and results in early embryonic lethality (Deans et al., 2000; Kuznetsov et al., 2009; Pittman and Schimenti, 2000; Shu et al., 1999). Haploinsufficiency has been observed in case of XRCC2 and Rad51B (Deans et al., 2003; Date et al., 2006) manifested by increased levels of chromosome aberrations and aneuploidy after exposure to DNA damaging agents. This indicates that proper expression levels of Rad51B and XRCC2 are essential for maintaining genomic stability. For the functional analysis of Rad51 paralogs in mammals hamster cell mutants have been instrumental. Mutant lines with defects in XRCC2, XRCC3 and Rad51C are moderately sensitive to ionizing radiation but extremely sensitive to DNA cross-linking

agents (Thacker, 2005). In addition, increased levels of chromosomal aberrations and mitotic centrosome numbers have been observed (French et al., 2002; Godthelp et al., 2002b; Griffin et al., 2000; Renglin et al., 2007; Liu et al., 1998).

The hamster mutant CL-V4B, which was characterized previously in our group, is defective in *Rad51C* (Godthelp et al., 2002b). Molecular analysis revealed the absence of exon 5 in mature Rad51C mRNA. Here we describe the characterization of two CL-V4B-derived revertant cell lines that display intermediate sensitivity to DNA damaging agents, increased frequencies of chromosomal aberrations, impaired sister chromatid cohesion and reduced cloning efficiency, suggesting haploinsufficiency of *Rad51C*. The causative mutation underlying the CL-V4B mutant phenotype was determined and mice were generated harboring an analogous splice site mutation. Heterozygous *Rad51C*^{splice} animals are viable and do not display any phenotypic abnormalities, but homozygous embryos die during early development.

MATERIALS AND METHODS

Cell culture and isolation of MMC-resistant revertants

The MMC-sensitive hamster cell mutant CL-V4B has been described previously (Godthelp et al., 2002b). To isolate independent MMC-resistant revertants, several cultures of 100-1000 cells were expanded to 10^7 cells and seeded at 1 x 10^5 cells in 94 mm dishes in the presence of 5 ng/ml mitomycin C (MMC; Kyowa). After 2 weeks, MMC-resistant clones were isolated and grown in the absence of MMC for further characterization. Hamster cells were cultured as described previously (Godthelp et al., 2002b).

Clonogenic survival assays

Cultures in exponential growth were trypsinized and 300-500 cells were plated in 94 mm dishes in duplicate (controls in triplicate), left to attach for 4 h, and then X-ray irradiated with a dose rate of 2.8 Gy/min (200 kV, 4 mA, 1 mm Al) or exposed to methyl methanesulfonate (MMS) for 1 h, to camptothecin and bleomycin for 24 h and continuously to MMC, in complete medium. After treatment with chemicals the cells were washed with PBS, and returned to fresh medium. After 8-10 days the dishes were rinsed with 0.9% NaCl, dried, stained with methylene blue (0.25%) and visible colonies were counted.

RT-PCR analysis

Total RNA was extracted using RNAzolB (Cinna/Biotecx Laboratories). Oligo-dT primed first strand cDNA was reverse transcribed from 2 µg RNA using the Riboclone cDNA synthesis system (Promega). Quantitative PCR reactions were carried out using the FastStart Universal SYBR Green Master (Rox) system (Roche) according to the manufacturer's instructions using primers 15 and 16 (located in exon 4 and exon 5, respectively) and 17 and 18 (located in exon 8 and exon 9, respectively). Real time amplifications were performed 3-6 times and normalized to the hypoxanthine-guanine phosphoribosyltransferase (HPRT)

housekeeping gene (primer pair 19-20). The absence of exon 5 in mutant *Rad51C* mRNA from *Rad51C*^{splice} embryos was shown by amplification using primer-pair F4-R1 spanning exons 4-9 as described previously (Godthelp et al., 2002b).

Immunofluorescence labeling and microscopy

For Rad51 foci analysis cells were grown on glass slides, giving sub-confluent cultures at the time of fixation. Cells were either mock-treated, treated with MMC (2.4 µg/ml for 1 h) or X-rays (12 Gy). Immunostaining and microscopy were performed as described previously (Godthelp et al., 2002b).

Immunoprecipitation

Total cell extracts were prepared by lysis of 10^7 exponentially growing hamster cells in 0.5 ml lysis buffer as described previously (Godthelp et al., 2002b). Rad51C was immunoprecipitated with rabbit anti-HsRad51C antibody (2287), proteins were separated on a 12% SDS-polyacrylamide gel, transferred to a PVDF-membrane (Millipore), and hybridized with mouse anti-HsRad51C antiserum (2H11, Novus) followed by a peroxidase-labelled anti-mouse antibody (Amersham). Antibody binding was detected by enhanced chemoluminescence (Amersham).

Analysis of chromosomal aberrations, sister chromatid exchanges and sister chromatid cohesion

Exponentially growing V79B, CL-V4B, V4B-MR1and V4B-MR2 cells were either mock-treated or treated for 2 h (for sister chromatid exchanges, SCEs) or 24 h (for chromosomal aberrations, CA) with MMC. Procedures for the analysis of SCEs, CAs and sister chromatid cohesion have been described previously (Godthelp et al., 2002b). Data for CAs and SCEs analyses are from at least two independent experiments of which the mean and the SEM were calculated.

Rad51C mutation in CL-V4B

Genomic DNA from CL-V4B and V79B wild type cells was amplified using exon 4 and exon 6 specific primers. Amplifications were performed using the Expand Long Template PCR system (Roche). The PCR conditions used were 2 min 94°C; 10 sec 94°C, 30 sec 63°C and 4 min 68°C for 10 cycles followed by 15 sec 94°C, 30 sec 63°C, 4 min 68°C for 25 cycles. After 10 cycles the polymerization time was increased by 20 sec in each cycle and after the last cycle with an additional 7 min. Amplified DNAs were gel-purified and sequenced using exon 5 specific primers.

Rad51C construct

The targeting construct was based on the ploxPneo vector, which contains a neomycin resistance marker flanked by lox sites and a thymidine kinase gene (Yang et al., 1998). Left and right arms were obtained by amplification of genomic DNA from 129/Ola-derived ES cells. A 7.8 kb fragment including exon 4-6 was amplified with primer 3 and

4 using an Expand Long Template PCR system (Roche) and an annealing temperature of 63°C. A 5.7 kb fragment containing exon 3 and 4 was amplified with primers 5 and 6, using an annealing temperature of 53°C. The 7.8 and 5.7 kb fragments were cloned into pCR®2.1-TOPO® using a TOPO® XL PCR Cloning kit (Invitrogen), resulting in TOPO/Rad51C$^{7.8kb}$ and TOPO/Rad51C$^{5.7kb}$, respectively. Exons and flanking sequences were verified by sequencing. The 7.8 kb fragment from TOPO/Rad51C$^{7.8kb}$ was excised by *Xba*I digestion, blunted and digested with *Not*I. A 5 kb terminal fragment was cloned in ploxPneo digested with *Not*I and *Hpa*I. To generate the left arm a 6.9 kb fragment was excised from TOPO/Rad51C$^{7.8kb}$ with *Cla*I and *Kpn*I and inserted into TOPO/Rad51C$^{5.7kb}$ digested with *Cla*I and *Kpn*I. From the resulting plasmid a 4.4 kb fragment was excised with *Xba*I and sub-cloned into pUC120. Using a GeneTailor Site-Directed Mutagenesis System (Invitrogen) a G->T splice site mutation was introduced at +5 of intron 5 with primers 13 and 14. After sequence verification the mutagenized fragment was excised with *Xba*I and cloned into the *Xba*I site of ploxPneo. A 6.2 kb *Bsh*TI fragment including the left arm was inserted into the ploxPneo construct containing the right arm and linearized with *Bsh*TI. Plasmid DNA was purified using an EndoFree Plasmid Maxi Kit (Qiagen) and linearized with *Not*I.

ES cells, electroporation and clonogenic survival

The 129/Ola derived IB10 ES cells (a subclone from E14 ES cells) were cultured as described previously (de Vries et al., 2005). 4x10^7 ES cells were resuspended in 800 µl PBS, containing 50 µg linearized targeting vector and electroporated at 800 V and a capacitance of 3 µF. Cells were seeded in six 94 mm dishes and after 24 and 72 h neomycin (175 µg/ml) and gancyclovir (1.3 µg/ml) were added, respectively. Resistant colonies were isolated after 10 days of selection, expanded and genomic DNA was analyzed by blot-hybridization. Left and right probe fragments were generated using primer sets 7-8 and 9-10, respectively. The presence of the splice site was confirmed by PCR using primers 11 and 12 followed by *Ssp*I digestion.

Clonogenic survival experiments were performed using wild type IB10 ES cells and heterozygous *Rad51C$^{splice/neo}$* ES cell clones 1-50 and 1-79 by seeding 500 cells on gelatin coated 94 mm dishes in 50% BRL-conditioned knock-out DMEM/50% fresh ES cell medium as described previously (de Waard et al., 2008). ES cells were left to attach for 16 h and thereafter treated for 1 h with different doses of MMC, washed with PBS, and grown for 8 days.

Targeted ES cells were microinjected into C57BL/6 blastocysts to generate chimeras, and chimeric males were mated with C57BL/6 females. Mice were genotyped by PCR using the primers lox51CM01, lox51CM02 and 51CMLNMP1. PCR conditions were as follows: 45 sec 94°C, 30 sec 60°C and 1 min 72°C. The wild type allele yields a fragment of 129 bp and the targeted allele a fragment of 184 bp. To remove the neomycin resistance marker, heterozygous *Rad51C$^{splice/neo}$* mice were crossed with EIIaCre mice (Williams-Simons and Westphal, 1999). Recombination between the

two lox sites yields a 179 bp product using primers lox51CM01 and lox51CM02. Accurate removal of the neomycin gene was confirmed by sequence analysis.

Primer sequences

primer 3: 5′-AGTTGCTGGCACAAGTCTAT-3′
primer 4: 5′-CTAATGCAGGAACAAGCAATGC-3′
primer 5: 5′-AATAAGCTTACTCAGGATACGAACGCAGGAGT-3′ (a 5′ *Hind*III site is underlined);
primer 6: 5′-ATAAAGCTTCAGGCTGACTATGGTAGCACAAG-3′ (a 5′ *Hind*III site is underlined);
primer 7: 5′-GCCTTGGAAACTCTACAAATTCTAA-3′;
primer 8: 5′-CACCAAACATGATTCAGAACTCTTCT-3′;
primer 9: 5′-CATGTGAGCTCTGGAAACTG-3′;
primer 10: 5′-CACCAATGCAGGAACAAGC-3′;
primer 11: 5′-CTTCTGTAAGAGCAGTGTAT-3′;
primer 12: 5′-CACTTGCCTA CCTATAATTC;
primer 13: 5′-GCAAATAATCACAGATTAGCTGTAAATATTATTGGCCAGGAG-3′ (the splice site mutation is underlined);
primer 14: 5′-CTCCTGGCCAATAATATTTACAGCTAATCTGTGATTATTTGC-3′ (the splice site mutation is underlined);
primer 15: 5′- GAGCTGCTGGCACAAGTCT-3′
primer 16: 5′-TCCGTCTATTATCACTAGCTGCAC-3′
primer 17: 5′-GGGGCATGCTGCTACAATAA-3′
primer 18 5′-GACTCCTTCTGGCTTGGTGA-3′
primer 19: 5′-TCCTCCTCAGACCGCTTTT-3′
primer 20: 5′-CCTGGTTCATCATCGCTAATC-3′
lox51CM01: 5′-TCAGTGGAAGGATGTGGCTG-3′;
lox51CM02: 5′-GGCTGCTGTATCAGTCCTAGA-3′;
51CMLNMP1: 5′-CCTACCCGGTAGAATTGACCTG-3′.

RESULTS

Identification of Rad51C mutation in CL-V4B

Analysis of CL-4VB mutant cells revealed an alternatively spliced Rad51C mRNA that lacks exon 5 (Godthelp et al., 2002b). Sequence analysis of a region encompassing exon 5 and flanking intronic sequences indicated a single GC->AT base pair change at position +5 of intron 5 in one of the two *Rad51C* alleles (Fig. 1). The G->A transition mutation is located near the 3′ end of the GT(A/G)AGT splice donor consensus sequence. As the wild type *Rad51C* allele in CL-V4B is presumably methylated and silenced (Jeggo and Holliday, 1986), the viability of CL-V4B cells is most likely due to a low level of correctly spliced Rad51C transcripts. RT-PCR amplification experiments

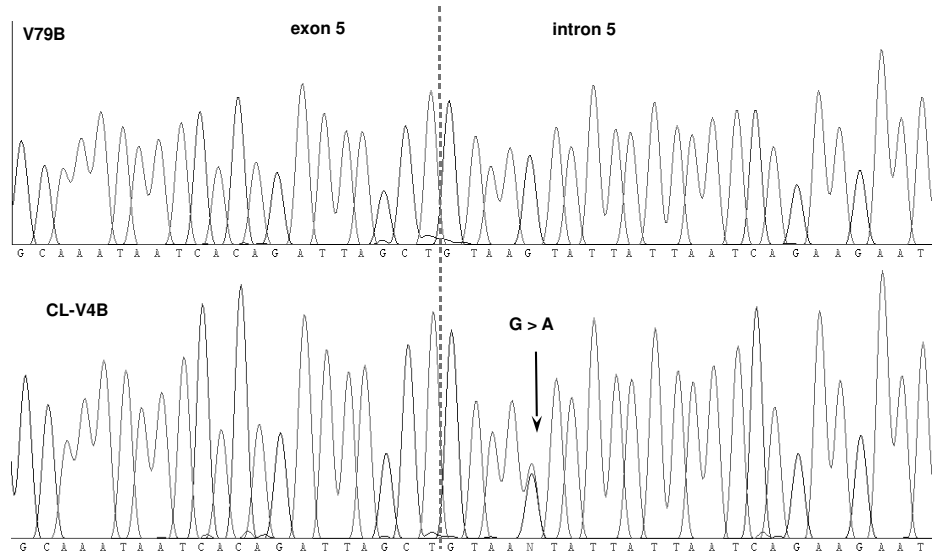

Figure 1. Sequence analysis of hamster *Rad51C*. Exon 5 and flanking regions were amplified using exon 4 and exon 6 specific primers and sequenced using exon 5 specific primers. Sequence traces illustrate the exon 5/intron 5 junctions of *Rad51C* of V79B (top) and CL-V4B (bottom) cells. The G>A transition at position +5 in one of the *Rad51C* alleles of CL-V4B is indicated by an arrow.

indeed showed a very low level of products of wild type length, although no Rad51C protein could be detected (results not shown; Fig. 2A).

MMC-resistant CL-V4B revertants display intermediate sensitivity to ICL-inducing agents in clonogenic survival and have a reduced cloning efficiency

CL-V4B hamster cells displayed an increased sensitivity towards various types of DNA damaging agents, especially to DNA cross-linking agents, like MMC (Godthelp et al., 2002b). Here, we describe the isolation and characterization of two independent MMC-resistant CL-V4B revertants, V4B-MR1 and V4B-MR2. Semi-quantitative PCR revealed that the level of full length Rad51C transcript was reduced in these revertants when compared to V79B (Fig. 2B) (Godthelp et al., 2002b). Sequence analysis indicated that both revertants still contain the splice donor mutation, suggesting that the wild type Rad51C allele is (partially) demethylated in these revertants. After immunoprecipitation Rad51C protein could be detected in both revertants, whereas Rad51C protein was below detection level in CL-V4B mutant cells (Fig. 2A).

The sensitivity of the V4B-MR1 and V4B-MR2 revertants to various DNA damaging agents was evaluated by clonogenic survival. Both revertants are still sensitive to the DNA interstrand cross-linking agent MMC (~ 2.6 fold), albeit much less than CL-V4B cells (~ 32-fold) (Fig. 3), based on the dose required to reduce the survival to 10%

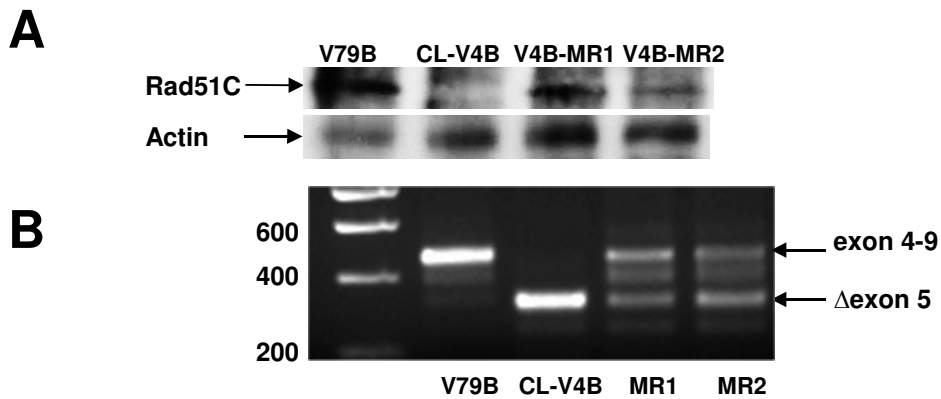

Figure 2. MMC-resistant CL-V4B revertants have reduced levels of full length Rad51C transcript and Rad51C protein. (A) The Rad51C protein was visualized by immunoprecipitation of cell lysates from V79B, CL-V4B, V4B-MR1 and V4B-MR2 cells using a polyclonal rabbit anti-hRad51C antibody followed by immunoblotting with a second anti-hRad51C antiserum. Equal loading was confirmed by hybridizing the IP-supernatant containing non-Rad51C bound proteins with a monoclonal antibody against actin. (B) Semi-quantitative RT-PCR of exon 4-9 of Rad51C using cDNA from wild type V79B, CL-V4B and CL-V4B revertants, V4B-MR1 and V4B-MR2, resulting in 457 (exon 4-9) and 325 bp (without exon 5) PCR fragments.

(D_{10}). The revertants were not sensitive to camptothecin, bleomycin or X-rays but are still slightly sensitive to the mono-functional alkylating agent MMS (~ 1.7-fold), although less than CL-V4B cells (~ 4-fold) (Fig. 3). The cloning efficiency of V4B-MR1 and V4B-MR2 in these experiments (57 ± 4.8% and 52 ± 5.6%, respectively) is in the same range as CL-V4B (58 ± 11 %) but is slightly reduced when compared to wild type V79B (73 ± 9 %). These results suggest Rad51C haploinsufficiency in the CL-V4B revertants due to reduced expression of the wild type *Rad51C* allele.

Intermediate levels of chromosomal aberrations, aberrant sister chromatid cohesion but normal levels of SCEs in CL-V4B revertants

We examined the spontaneous as well as the MMC-induced chromosomal aberrations (CAs) in the CL-V4B revertants, V4B-MR1 and V4B-MR2, to establish if both lines still display genomic instability as was observed in CL-V4B cells (Godthelp et al., 2002b). This analysis revealed that V4B-MR1 and V4B–MR2 show a 4-fold higher level of spontaneous CAs and a 2-fold higher level of MMC-induced CAs when compared to wild type V79B cells but less than in CL-V4B (29- and 100-fold, respectively) (Table 1A/B).

Next we investigated sister chromatid cohesion in metaphase spreads of both CL-V4B revertants since reduced levels of sister chromatid cohesion were found in Rad51C mutant CL-V4B (Godthelp et al., 2002b). Microscopic analysis revealed that in V4B-MR1 and V4B-MR2 the number of cells showing separated chromatids was 1.6 fold increased when compared to wild type V79B cells,

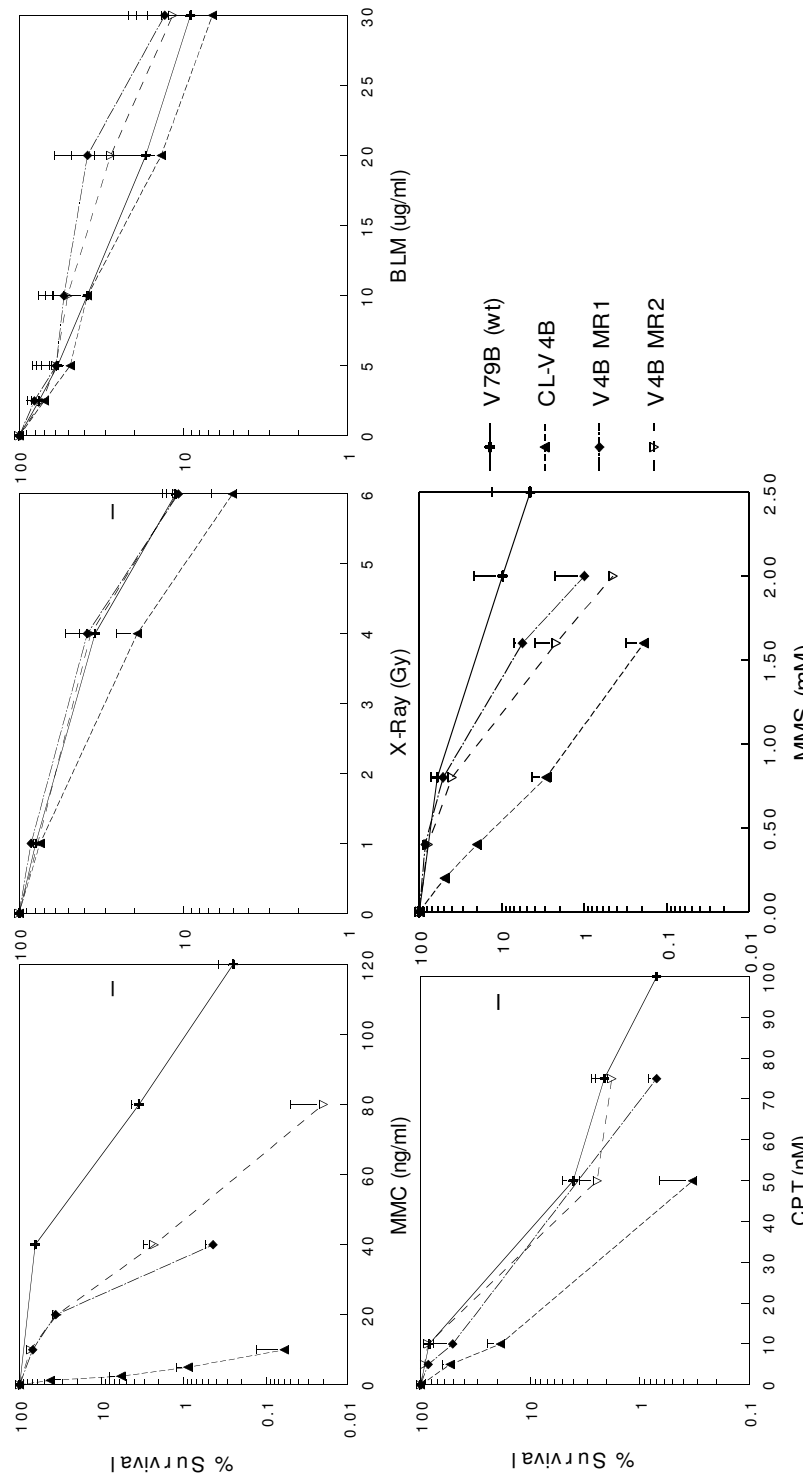

Figure 3. CL-V4B revertants, V4B-MR1 and V4B-MR2, remain sensitive for DNA ICL-inducing agents and MMS. Clonogenic survival of CL-V4B, V4B-MR1, V4B-MR2 and parental V79B cells after exposure to MMC, camptothecin (CPT), MMS, bleomycin (BLM) and after irradiation with X-rays. Data are the means of at least 3 experiments. Error bars represent the standard error of the mean (SEM).

whereas CL-V4B cells showed a 2-3 fold increase in cells with precocious sister chromatid separation (Table 1A). Together the analysis of CAs and sister chromatid cohesion also suggest haploinsufficiency of Rad51C in both revertants, which is in concordance with the survival experiments.

Since CL-V4B cells were also shown to be severely hampered in MMC-induced sister chromatid exchange (SCE) formation (Godthelp et al., 2002b), we analyzed the levels of SCE induction in V4B-MR1 and V4B-MR2. The data shown in Fig. 4A indicate normal frequencies of SCEs both spontaneous (3.8 and 3.4 SCE/cell, respectively) as well as after MMC treatment (10.2 and 10.1 SCE/cell at 30 ng/ml MMC) in these revertants, when compared to wild type V79B cells (4.3 SCE/cell spontaneous and 11.5 SCE/cells after 30 ng/ml MMC).

CL-V4B revertants display a normal DNA damage induced Rad51 foci phenotype

The inactivation of *Rad51C* causes a severe defect in the formation of DNA damage induced Rad51 foci in CL-V4B mutant cells (Godthelp et al., 2002b). In V4B-MR1 and V4B-MR2 the induction of Rad51 foci after MMC treatment or X-ray irradiation was restored to near wild type levels (Fig. 4B). Moreover, the dynamics of Rad51 foci formation after X-ray irradiation as well as the number of Rad51 foci per nucleus in these revertants was also comparable to wild type cells (Fig. 4B; results not shown). However, after MMC treatment the disappearance of Rad51 foci seemed to be somewhat slower in the revertants when compared to wild type cells. These data indicate that the expression level of Rad51C in the revertants is adequate for sequestration of Rad51 into nuclear foci and for the normal induction of SCEs after exposure to DNA damaging agents.

Generation of Rad51C mutant mice

To mimic the CL-V4B Rad51C mutation in mice, a targeting construct was generated containing a GC->AT change at position +5 of intron 5. The nucleotide and protein sequences of Rad51C are strongly conserved between hamster and mouse. The first 12 nucleotides of intron 5 are identical between both organisms and up to position +40 only 7 base pair changes were detected. The targeting vector was linearized with *Not*I and electroporated into ES cells (Fig. 5A). We tested ~250 neomycin- and gangcyclovir-resistant ES cell clones by blot-hybridization for correct targeting. Correct targeting resulted in a novel 10.5 kb *Pvu*II fragment on the left and a novel 6.0 kb *Sph*I fragment on the right and was seen in clones 1-79 (data not shown) and 1-50 (Fig. 5B). The presence of the G->A splice site in correctly targeted cells was confirmed by PCR and *Ssp*I digestion (Fig. 5C). RNA isolated from wild type and *Rad51C*$^{splice/neo}$ ES cells was analyzed by quantitative PCR. Together, the results obtained using two primer sets indicate a reduction of 40-50% in the level of full length Rad51C mRNA in both ES cell clones (Fig. 5D). Targeted ES cells were injected into C57BL/6 blastocysts and germ line transmitting animals were obtained.

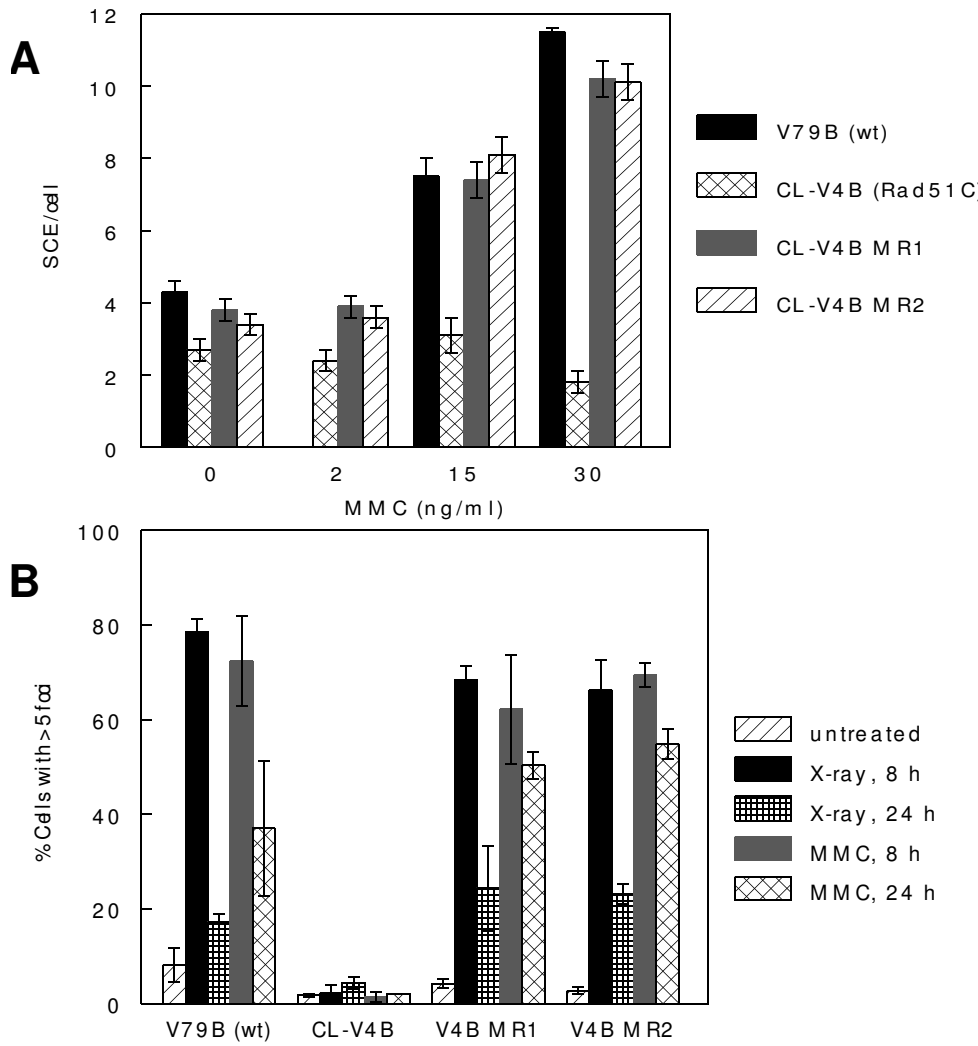

Figure 4. Normal DNA damage induced Rad51 foci formation and SCE induction in CL-V4B revertants. (A) SCE formation after MMC treatment. V79B, CL-V4B, V4B-MR1 and V4B-MR2 cells were either mock-treated or treated with various MMC doses (2, 15 and 30 ng/ml for V4B, V4B-MR1, V4B-MR2 and 15 and 20 ng/ml for V79B) before SCE visualization. Data are the mean of at least two independent experiments; error bars represent the SEM. (B) Kinetics of Rad51 foci formation in V79B, CL-V4B, V4B-MR1 and V4B-MR2 cells analyzed 8 and 24 h after treatment with MMC (2.4 μg/ml for 1 h) or after X-ray irradiation (12 Gy). Cells containing more than 5 distinct foci in the nucleus were considered to be positive. Data are the means of at least 2 experiments. Error bars represent the SEM.

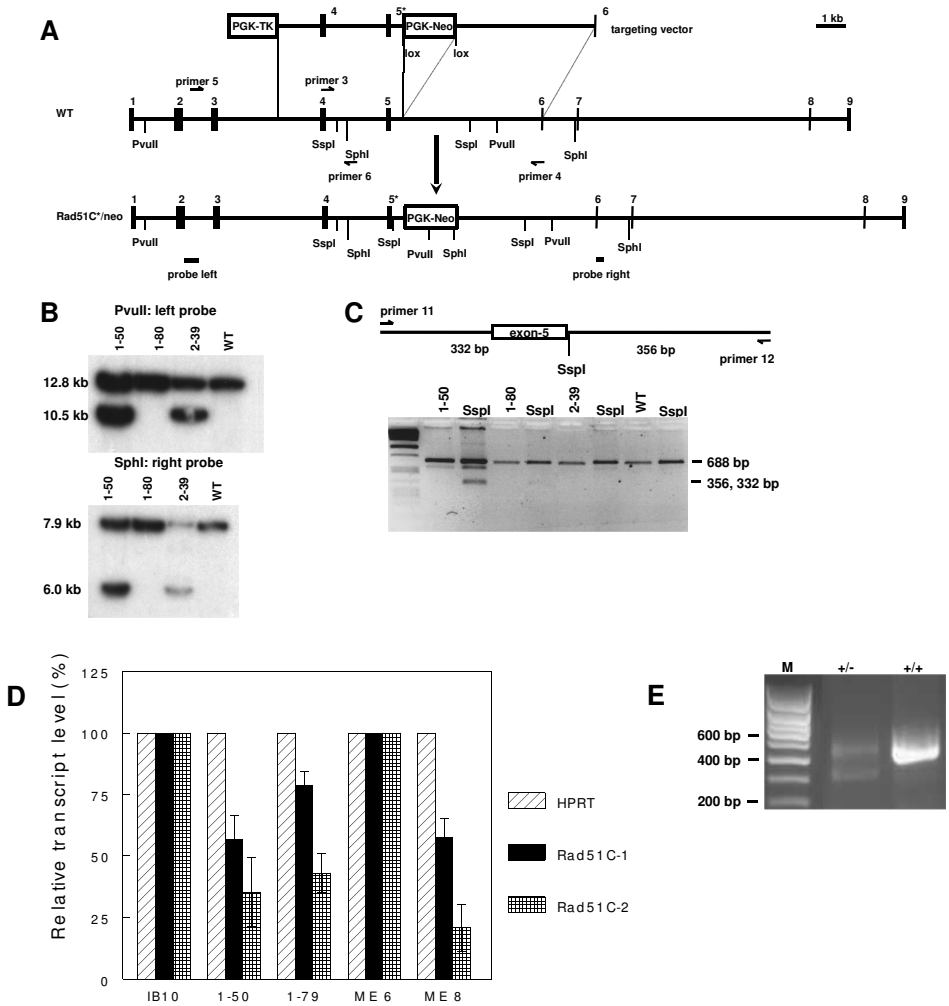

Figure 5. Rad51C targeting construct. (A) Schematic representation of the targeting vector, the mouse *Rad51C* locus and the targeted locus. Exons are indicated by solid boxes. The presence of the G>A splice site mutation at position +5 of intron 5 is indicated by the asterisk (B) Blot-analysis of DNA from neomycin resistant clones and wild type ES cells digested with *Pvu*II (top) and *Sph*I (bottom) and hybridized with left and right probes, respectively. (C) PCR analysis followed by *Ssp*I digestion to confirm the GC>AT base pair substitution. The presence of the splice site mutation results in the formation of a novel *Ssp*I site (AGTATT>AATATT). The data indicate correct targeting in clone 1-50, random integration in clone 1-80 and correct targeting but loss of the splice site mutation in clone 2-39. (D) Quantitative PCR analysis of RNA isolated from wild type IB10 ES cells, 1-50 *Rad51C*$^{splice/neo}$ ES cells, 1-79 *Rad51C*$^{splice/neo}$ ES cells, wild type embryos (ME 6) and heterozygous *Rad51C*^{splice} embryos (ME 8) using HPRT (primer 19-20), Rad51C-1 (primer 15-16) and Rad51C-2 (primer 17-18) primer pairs. Data were normalized to the HPRT housekeeping gene. Error bars represent the SD. (E) RT-PCR analysis of RNA from heterozygous and homozygous embryos. Using exon 4 and exon 9 specific primers a wild type fragment of 457 bp is obtained and a 325 bp fragment after loss of exon 5.

Mice heterozygous for the *Rad51C*$^{splice/neo}$ mutation show no gross abnormalities and their viability was not affected. However, intercrosses failed to produce viable homozygous mutant offspring. Among 63 pups genotyped by PCR, 42 were heterozygous and 21 were wild type indicating that homozygosity of the *Rad51C*$^{splice/neo}$ mutation results in embryonic lethality. In CL-V4B cells the presence of a G->A transition mutation results in aberrantly spliced Rad51C mRNA molecules which lack exon 5. RT-PCR analysis using exon 4 and 9 specific primers, however, only showed products of wild type length in heterozygous *Rad51C*$^{splice/neo}$ ES cells (results not shown). Most likely the presence of the neomycin resistance marker, which is transcribed in the opposite direction, interferes with transcription of the *Rad51C* gene and results in a null allele.

To mimic the situation in CL-V4B cells the neomycin gene was removed by crossing *Rad51C*$^{splice/neo}$ animals to EIIaCre mice. RT-PCR analysis showed the presence of a 457 bp Rad51C product in wild type embryos using exon 4 and exon 9 specific primers (Fig. 5E). In heterozygous embryos also a product of 325 bp was detected which is indicative for aberrantly spliced Rad51C mRNA molecules lacking exon 5, as was observed previously in CL-V4B hamster cells. Quantitative PCR analysis using two primer sets indicated a reduction of approximately 60% in the level of wild type Rad51C mRNA in heterozygous *Rad51C*^{splice} embryos (Fig. 5D).

Rad51C$^{splice/neo}$ and *Rad51C*^{splice} mutant strains were maintained by backcrossing to C57BL/6J animals. Heterozygous offspring was obtained in a normal Mendelian fashion. In the course of the study presented here 172 *Rad51C*$^{splice/neo}$ and 153 *Rad51C*^{splice} heterozygous animals were recovered. Visual inspection, up to 6-7 months of age, did not reveal any noticeable abnormalities or an increase in spontaneous tumor formation in comparison to wild type littermates.

To ascertain if homozygous mutant animals could be obtained, heterozygous *Rad51C*^{splice} animals were interbred and of 70 pups analyzed 47 were heterozygous and 23 wild type. No viable homozygous mutants were recovered, indicating that homozygosity for the *Rad51C*^{splice} mutation leads to embryonic lethality. To determine at which developmental stage lethality occurs, timed matings were performed and embryos were genotyped at different stages of gestation. No homozygous mutant embryos were found at embryonic day 12.5 (E12.5) and E10. However, at E8.5 homozygous *Rad51C*^{splice} embryos were present at a frequency of 23%. Most E8.5 homozygous mutant embryos were smaller in size when compared with heterozygous embryos and started to degenerate.

Rad51C$^{splice/neo}$ heterozygous ES cells are sensitive to MMC

To investigate whether *Rad51C*$^{splice/neo}$ heterozygous ES cells are more sensitive to ICL inducing agents than wild type cells we compared the MMC sensitivity of heterozygous clones 1-50 and 1-79 to wild type IB10 cells. As shown in Fig. 6, *Rad51C*$^{splice/neo}$ heterozygous ES cell clones 1-50 and 1-79 are 1.4 fold more sensitive to MMC than wild type ES cells. These data indicate that Rad51C haploinsufficiency

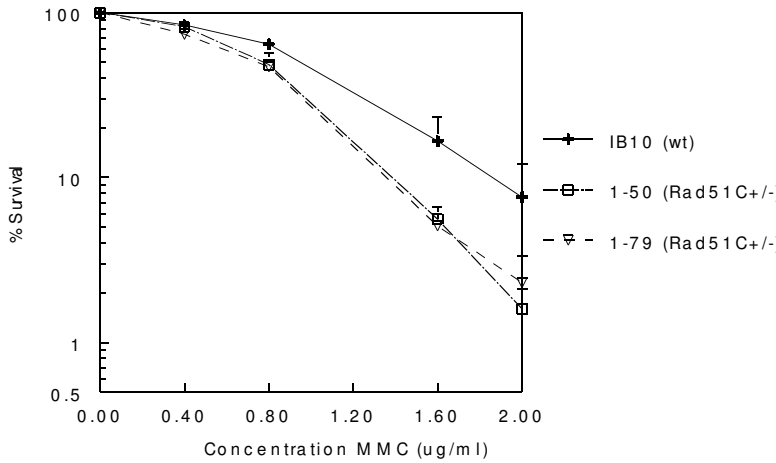

Figure 6. *Rad51C*^{splice}/neo heterozygous ES cells are sensitive to MMC.Clonogenic survival of Rad51C heterozygous ES cell clones 1-79, 1-50 and wild type IB10 ES cells after exposure to MMC. Data are the means of at least 4 experiments. Error bars represent the standard error of the mean (SEM).

also gives rise to ICL sensitivity in mouse ES cells, which is in concordance with our observations in the CL-V4B revertants.

DISCUSSION

In the present study we have shown that the *Rad51C* splice donor mutation of CL-V4B gives rise to embryonic lethality in mice and that haploinsufficiency of *Rad51C* leads to MMC sensitivity in hamster cell revertants V4B-MR1 and V4B-MR2 as well as in heterozygous *Rad51C*$^{splice/neo}$ mouse ES clones. Moreover, *Rad51C* haploinsufficiency also gives rise to increased frequencies of spontaneous and MMC-induced CAs, impaired sister chromatid cohesion and reduced cloning efficiency in hamster revertants V4B-MR1 and V4B-MR2.

Although, we formally cannot exclude the possibility that there may be a negative effect of the mutant Rad51C protein lacking exon 5, this does not seem very likely as both revertants show normal induction of Rad51 foci and SCEs in response to DNA damaging agents. Apparently, the level of Rad51C protein in both revertants is sufficient for SCE induction and Rad51 foci formation after infliction of damage but not for preventing enhanced formation of spontaneous and MMC-induced chromosomal aberrations. Similarly, XRCC2 or Rad51B haploinsufficiency gives rise to increased levels of CAs but levels of Rad51 foci after DNA damage are near normal (Deans et al., 2003; Date et al., 2006). In contrast, *Rad51C*$^{ko/+}$ MEFs (Kuznetsov et al., 2009) did not show an increased level of CAs at low passage number after treatment with a single dose of MMC when compared to wild type MEFs. This difference might

be cell type specific or related to the MMC dose and/or the single time-point of fixation used in this paper.

Homozygosity for the CL-V4B splice site mutation leads to early embryonic lethality in mice. Aberrant splicing of Rad51C mRNA leading to loss of exon 5 is apparently not compatible with embryonic development. This is in concordance with data from Kuznetsov *et al*. (Kuznetsov et al., 2009) showing embryonic lethality of *Rad51C*^{null} alleles. Like *Rad51C*, loss of other *Rad51* paralogs also results in early embryonic lethality. Inactivation of *Rad51B*^{null} leads to the most severe phenotype as mutant embryos disappear at E7.5 (Shu et al., 1999). *Rad51D*-deficient embryos die between E8.5 and E11.5 (Pittman and Schimenti, 2000) and *XRCC2* mutant embryos between E10.5 and E12.5 (Deans et al., 2000). *Rad51C*^{null} and *Rad51D*^{null} heterozygous mice did not show increased tumorigenesis, showing that heterozygosity for *Rad51C* or *Rad51D* alone does not predispose mice to cancer (Kuznetsov et al., 2009; Pittman and Schimenti, 2000). Up to 6-7 months of age we also did not observe an increase in tumor formation in heterozygous *Rad51C*$^{splice/neo}$ or *Rad51C*^{splice} animals. However, Rad51C heterozygosity leads to modulation of Trp53-dependent tumor formation in epithelial tissues such as sebaceous glands as observed in Rad51C^{null}p53^{null} double heterozygous mice (Kuznetsov et al., 2009). Whether heterozygous *Rad51C*^{splice} mice also display increased Trp53-dependent tumorigenesis in epithelial tissues remains to be ascertained.

Why is the *Rad51C* splice site mutation tolerated in hamster cells and not during embryonic development in mice? As exon 5 codes for a conserved region of Rad51C containing the Walker B ATP binding motif, it is not very likely that lack of exon 5 results in a functional protein. Most probably the viability of CL-V4B cells is due to a very low level of correctly spliced Rad51C mRNA and/or a low level of expression of the second *Rad51C* allele, which may not be completely silenced by methylation. As the effects of splice site mutations can be cell-type or species specific, we cannot exclude the possibility that the GC->AT transition at position +5 of intron 5 of *Rad51C* has a more severe effect on splicing in mouse embryonic cells as compared with hamster lung fibroblasts. The results obtained indicate that the residual level of full-length Rad51C protein is sufficient in cultured hamster cells but not in rapidly developing embryos. However, when challenged by DNA damaging agents, repair is severely hampered in CL-V4B cells as a consequence of very low levels of full-length Rad51C transcript.

Haploinsufficiency has been reported for Rad51 paralogs such as *XRCC2* and *Rad51B* (Deans et al., 2003; Date et al., 2006) and for other genes involved in the DNA damage response (DDR) such as BRCA1, BRCA2, Rad50 and NBS1 (Heikkinen et al., 2006; Jeng et al., 2007; Wiegant et al., 2006). Haploinsufficiency in DDR genes causes genomic instability and may therefore provide a selective advantage that could lead to clonal expansion and tumor promotion (Quon and Berns, 2001). It has even been proposed that DDR functions as a biological tumorigenesis barrier in early stages of cancer development favoring outgrowth of malignant clones with defects in the genome maintenance machinery (Kelemen et al., 2009). The recent discovery of pathogenic *Rad51C* mutations in German hereditary breast and ovarian cancer families (Kelemen et al., 2009; Meindl et al., 2010) and of biallelic germline

Rad51C mutations in a Fanconi anemia like syndrome (Vaz et al., 2010) emphasizes the cancer proneness of individuals with reduced *Rad51C* expression.

The chromosomal region containing *Rad51C* has commonly found to be amplified in sporadic breast cancers. This amplification was associated with over-expression of Rad51C as well as several other linked genes in a significant proportion of primary tumors (Kelemen et al., 2009; Parssinen et al., 2007; Sinclair et al., 2003). In the MCF7 breast cancer cell line a breakpoint was identified in the *Rad51C* gene resulting in a Rad51C-ATXN7 fusion product. As a consequence the interaction of Rad51C with other Rad51 paralogs is disrupted, suggesting that Rad51C might be involved in cancer progression (Hampton et al., 2009). In mice, loss of Rad51C leads to modulation of Trp53-dependent tumorigenesis, indicating that Rad51C might function as a tumor suppressor (Kuznetsov et al., 2009).

Cohesion between sister chromatids is mediated by the multisubunit cohesin complex that is also implicated in repair of damaged DNA and in regulation of gene expression (Peters et al., 2008). The data presented in this paper indicate that *Rad51C* haploinsufficiency influences sister chromatid cohesion but whether this is due to a direct interaction of Rad51C with the cohesin complex and its interacting proteins or a consequence of defects in HR remains to be established. The observation of impaired sister chromatid cohesion in CL-V4B revertants is in concordance with data obtained with mouse oocytes expressing a hypomorphic *Rad51C* allele (resulting in reduced expression in some of the animals) that also exhibit a sister chromatid cohesion defect (Kuznetsov et al., 2007). Impaired sister chromatid cohesion might cause aneuploidy which may link cohesion defects to tumorigenesis (Panigrahi and Pati, 2009). Haploinsufficiency of *Rad51C* may therefore contribute to tumorigenesis not only by increased genomic instability as a consequence of defects in repair but also through inappropriate cohesion between sister chromatids.

CONFLICT OF INTEREST STATEMENT

The authors declare that there are no conflicts of interest.

ACKNOWLEDGEMENTS

We thank F.E. Benson and R. Kanaar for providing us with Rad51 (FBE2) and Rad51C (2287) antibodies and Chu-Xia Deng for providing us with the ploxPneo vector. We are indebted to the Central Mouse Facility at the LUMC for blastocyst injections and general mouse facilities. We also would like to thank L. Wetselaar, D. Krijgsman and M. Dijkstra for their skilful technical assistance. This work was supported, in part, by the Netherlands Organization for Scientific Research (NWO, grant 901-01-190) and the EU (RISC-RAD project: FI6R-CT-2003-508842 and DNA repair project: LSHG-CT-2005-512113).

Table 1A. Spontaneous, MMC-induced chromosomal aberrations (CA) and premature sister chromatid separation per 100 cells

Cell line	MMC dose	Cells with CA	Chromatid Breaks	Exchanges[a]	Total breaks[b] ± SEM	Cells with premature SCS[c] ± SEM
V79B	Spontaneous	2	2	0	2 ± 0	41 ± 4
	80 ng/ml	24	65	5	70 ±15	
CL-V4B	Spontaneous	29	51	6	57 ± 11	79 ± 3
	2 ng/ml	79	159	67	225 ±18	
V4B-MR1	Spontaneous	7	7	1	8 ± 3	65 ± 3
	2 ng/ml	11	27	1	28 ± 6	
	40 ng/ml	40	62	11	73 ± 4	
	80 ng/ml	54	117	29	146 ± 1	
V4B-MR2	Spontaneous	7	7	1	8 ± 3	70 ± 5
	2ng/ml	12	16	2	18 ± 2	
	40 ng/ml	32	52	6	58 ± 1	
	80 ng/ml	54	173	16	189 ± 15	

Table 1B. Relative sensitivities for chromosomal aberrations

	Relative Sensitivity			
	V79B	CL-V4B	V4B-MR1	V4B-MR2
Spontaneous	1[d]	29	4	4
MMC-induced	1[e]	100	2	2

[a] Chromatid exchanges are interchanges, intrachanges, triradials or subchromatid exchanges.
[b] For calculations of the total number of breaks, the breaks and exchanges were counted as 1 break since dose-response relationships for MMC-induced exchange configurations were linear [48].
[c] SCS, sister chromatid separation.
[d] The frequency of spontaneous aberrations per 100 cells in parental V79B cells was 2 ± 0 and this was set at 1.
[e] The slope of the induction curve of CA after MMC-treatment in parental V79B cells was 0.4 aberrations per 100 cells per ng/ml MMC, and this was set as 1. All slopes were determined by using at least 3 different dose levels.